DOI: 10.1002/chem.200902977

Electron Attachment to Hydrated Oligonucleotide Dimers: Guanylyl-3′,5′-Cytidine and Cytidylyl-3′,5′-Guanosine

Jiande Gu,*[a] Yaoming Xie,[b] and Henry F. Schaefer, III*[b]

Abstract: The dinucleoside phosphate deoxycytidylyl-3′,5′-deoxyguanosine (dCpdG) and deoxyguanylyl-3′,5′-deoxycytidine (dGpdC) systems are among the largest to be studied by reliable theoretical methods. Exploring electron attachment to these subunits of DNA single strands provides significant progress toward definitive predictions of the electron affinities of DNA single strands. The adiabatic electron affinities of the oligonucleotides are found to be sequence dependent. Deoxycytidine (dC) on the 5′ end, dCpdG, has larger adiabatic electron affinity (AEA, 0.90 eV) than dC on the 3′ end of the oligomer (dGpdC, 0.66 eV). The geometric features, molecular orbital analyses, and charge distribution studies for the radical anions of the cytidine-containing oligonucleotides demonstrate that the excess electron in these anionic systems is dominantly located on the cytosine nucleobase moiety. The π-stacking interaction between nucleobases G and C seems unlikely to improve the electron-capturing ability of the oligonucleotide dimers. The influence of the neighboring base on the electron-capturing ability of cytosine should be attributed to the intensified proton accepting–donating interaction between the bases. The present investigation demonstrates that the vertical detachment energies (VDEs) of the radical anions of the oligonucleotides dGpdC and dCpdG are significantly larger than those of the corresponding nucleotides. Consequently, reactions with low activation barriers, such as those for O–C σ bond and N-glycosidic bond breakage, might be expected for the radical anions of the guanosine–cytosine mixed oligonucleotides.

Keywords: density functional calculations · DNA · electron affinity · oligonucleotides · radical ions

Introduction

Electron attachment to DNA fragments is one of the most attractive subjects in both radiation biology[1–4] and functional nanomaterial science.[5–8] Knowledge of the distribution of excess electron sites for DNA strands is crucial for understanding important biochemical processes, such as anion-related DNA damage and repair,[1,9–17] charge transfer,[5–7,18–23] and mutations.[9,11,24] Moreover, the electron-accepting ability of the different subunits of DNA is one of the keystones of the creation of DNA-inspired electronically active materials.[8]

Direct experimental characterization of electron attachment to DNA strands and DNA fragments may be traced back to 1990.[25,26] Later experiments suggest that the pyrimidine nucleobases have small electron affinities (EAs), ≈0.1 eV for thymine (T), cytosine (C), and uracil (U).[27,28] Negative EA values have been deduced for adenine (A) and C from gas-phase experiments.[29–32] Recently, photoelectron spectroscopy has detected bound anionic states of adenine and guanine tautomers that have relatively large vertical electron detachment energies.[32,33] The photoelectron spectra of the anionic base pairs of adenine and thymine ($AT^{\bullet-}$) and 9-methyladenine and 1-methylthymine ($mAmT^{\bullet-}$) yielded vertical detachment energies (VDEs) of 1.7 eV for the former and 0.7 eV for the latter.[34] Compared to the reliable theoretical prediction of the VDE of the canonical form of radical anion $AT^{\bullet-}$ (0.64 eV),[35] the large VDE reported for $AT^{\bullet-}$ strongly suggests that this base pair adopts a tautomeric form under the experimental conditions. Electron attachment energies of the radical anions of nucleosides have also

[a] Prof. J. Gu
Drug Design & Discovery Center
State Key Laboratory of Drug Research
Shanghai Institute of Materia Medica
Shanghai Institutes for Biological Sciences, CAS
Shanghai 201203 (P. R. China)
Fax: (+86) 21-508-066-00
E-mail: jiandegush@go.com

[b] Dr. Y. Xie, Prof. H. F. Schaefer, III
Center for Computational Quantum Chemistry
University of Georgia, Athens
Georgia 30602-2525 (USA)
E-mail: sch@uga.edu

been determined by Bowen's group.[36] These experimental electron affinity values, for thymidine, cytidine, and adenosine, are within 0.2 eV of the previously reported theoretical predictions.[37] However, experiments on the electron-capturing efficiencies of short DNA oligomers provide the only estimate of the relative order of the vertical electron attachment energies (VEAs) for DNA single strands.[4]

Theoretical investigations at various levels of sophistication have been complemented with experimental explorations. The coupled cluster level of theory with single, double, and perturbative triple excitations (CCSD(T)) successfully elucidated the tautomeric forms of the covalent bond radical anion of guanine[33,38] and adenine.[32] The best density functional theory (DFT) approaches yield adiabatic electron affinities (AEAs) of individual nucleic acid bases that are consistent with the best experiments.[39–41] Step by step, with the extensively calibrated B3LYP/DZP++ approach,[42] a trustable data bank of the electron affinities of the 2′-deoxyribonucleosides (the predicted AEA and VDEs have recently been confirmed by photoelectron spectroscopic experiments),[36,37] the nucleotides (3′-dCMP, 3′-dTMP, 5′-dCMP, 5′-dTMP),[43–47] and the nucleoside-3′,5′-diphosphates (3′,5′-dGDP, 3′,5′-dADP, 3′,5′-dCDP, and 3′,5′-dTDP)[48] has been established. Theoretical studies of electron attachment to DNA have been extended to the prediction of the electron affinities of the hydrogen-bonding paired DNA subunits, such as nucleobase pairs[34,49–52] (A:T and G:C pair, first reported by Sevilla's group[49,50]), the nucleoside pairs (dA:dT and dG:dC),[53,54] and at least one nucleotide—nucleobase pair.[55] The DFT approach has also been applied to elucidate the electron-capturing abilities of the A:T pair and the mA:mT pair in their tautomeric forms by Radisic et al.[34] The influence of water microsolvation on the electron attachment to nucleobases has also been investigated extensively at different levels of theory.[56–69] Recently, the electron affinities of the thymine-adenine base-pair stacking between different bases were studied by the "resolution of identity formulation of MP2" (RI-MP2) approach.[70] These investigations suggest that the pyrimidines in DNA fragments have a strong tendency to capture low-energy electrons and to form electronically stable radical anions. Both the presence of the ribose and phosphate backbones in DNA strands and water microsolvation greatly increase the electron affinities of the nucleobases.

Along with the effects of the ribose and phosphate backbones in DNA, the influence of the stacked neighboring bases has been revealed, first by Simons' group,[71] to be an important factor for the electron-capturing ability of DNA single strands. As a further step to achieving a realistic description of the electron attachment to the nucleotide oligomers, dinucleoside phosphate deoxycytidylyl-3′,5′-deoxyguanosine (dCpdG) and deoxyguanylyl-3′,5′-deoxycytidine (dGpdC) and the corresponding radical anions ([dCpdG]$^{\bullet-}$ and [dGpdC]$^{\bullet-}$) have been investigated theoretically in our laboratories. To include the important effects of water microsolvation on the electron affinities of the nucleobases, four water molecules are also appended to each oligonucleotide dimer. These systems represent the most complete descriptions to date of the minimum length of chain in a single strand of DNA and are keystones for understanding electron attachment to single-strand DNA.

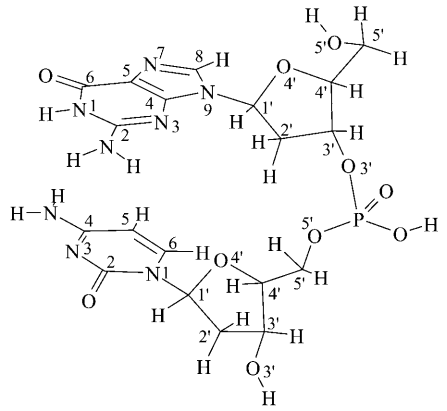

dGpdC

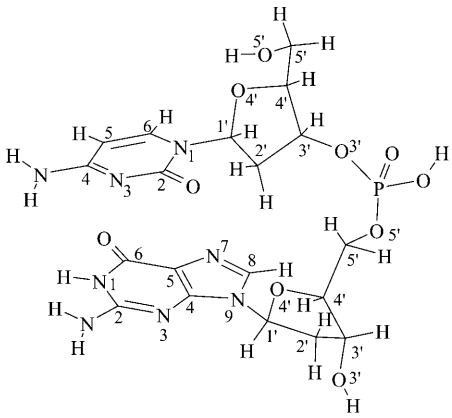

dCpdG

Computational Methods

Three functionals, B3LYP,[72,73] BH&H,[74] and M05-2X,[75,76] with basis sets of double-ζ quality plus polarization and diffuse functions (denoted DZP++), were used to obtain optimized geometries and to evaluate energetics and natural charges for the DNA subunits in both neutral and anionic forms. The DZP++ basis sets were constructed by augmenting the Huzinaga-Dunning[77] set of contracted double-ζ gaussian functions. To complete the DZP++ basis, one even-tempered diffuse s function was added to each H atom, and sets of even-tempered diffuse s and p functions were centered on each heavy atom. The even-tempered orbital exponents were determined according to the prescription of Lee and Schaefer.[78] Each adiabatic electron affinity (AEA) was computed as the difference between the absolute energies of the appropriate neutral and anionic species at their respective optimized geometries: AEA = $E_{neutral} - E_{anion}$.

Four water molecules are appended to each oligonucleotide dimer in order to examine the important effects of water microsolvation on the electron affinities of the nucleobase. Earlier experiments have demonstrated that the presence of the microsolvation water molecules is able to transfer the dipole-bound radical anions of nucleobases into covalent radical anions.[27,53] To further evaluate the electron-capturing abilities of

DNA single strands in aqueous solution, a polarizable continuum model (PCM)[79] with water dielectric constant ($\varepsilon = 78.39$) was used to simulate the solvated environment of an aqueous solution. Natural population analyses (NPA) were determined using the three mentioned functionals and the DZP++ basis set with the natural bond orbital (NBO) analysis of Reed and Weinhold.[80,81] The Gaussian 03[82] system of DFT programs was used for all computations.

Among the three functionals, B3LYP has a long track record in successfully reproduced, experimentally consistent, electron affinities of nucleobases,[39–41] and has predicted the electron affinities of other DNA subunits, which have been confirmed by recent experiments.[36,37] It is known that conventional DFT methods, such as B3LYP, do not provide a correct description of the interactions resulting from the dispersion. Therefore, structures with pure stacked nucleobases do not correspond to the local minima on the potential energy surface provided by the B3LYP approach. However, owing to the fact that nucleobases are both good proton acceptors and donors, the microsolvating water molecules might be able to "lock" the bases in the stacked forms through the formation of a hydrogen-bonding network with the bases. On the other hand, the newly-developed functional M05-2X has been tested successfully for systems with non-covalent weak interactions, including systems with important contributions from dispersion.[75,76] Meanwhile, the "old" functional, BH&H, has also been found to be reasonably good in describing π-stacking systems.[83] Therefore, these two functionals were also adopted in the present study. It should be noted that although second-order Møller-Plesset perturbation (MP2) may provide a better theoretical description of base-stacking interactions, the serious underestimation of the adiabatic electron affinities of the nucleobases[84–86] make it impractical for electron attachment studies of systems such as oligonucleotide dimers.

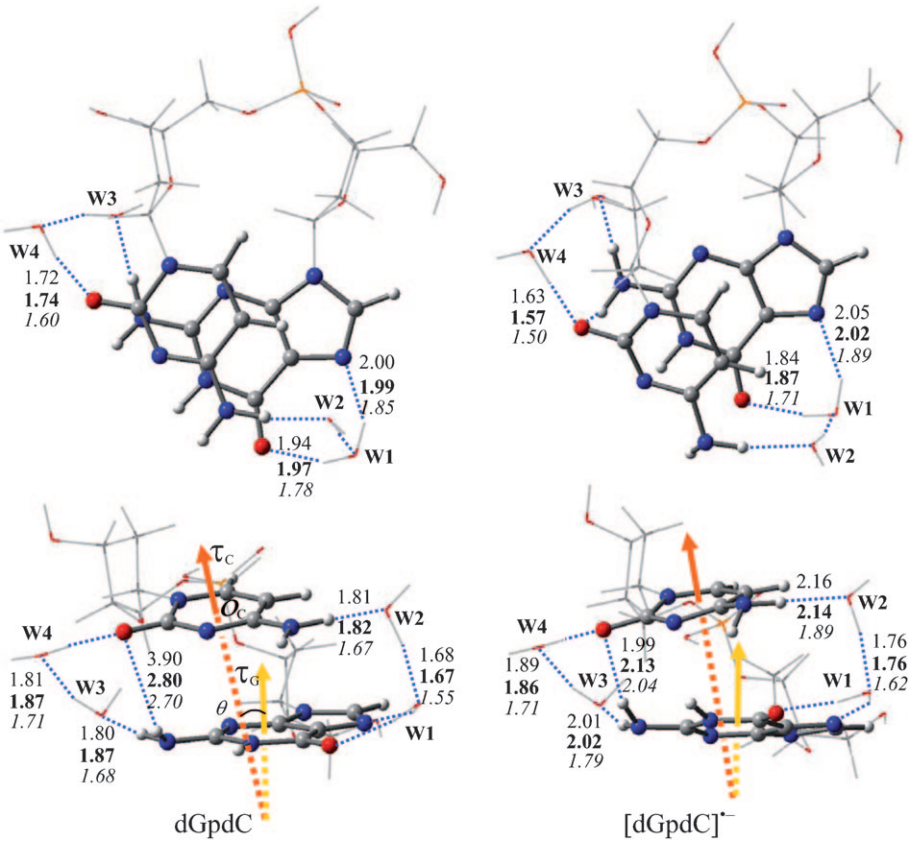

Figure 1. Optimized geometrical structures for the neutral molecules and radical anions of the water microsolvated dGpdC. Bond lengths are in Å. Color representations: orange for P, gray for C, red for O, blue for N, and white for H. The thin lines represent the riboses, the phosphates, and the hydration water molecules. Bond lengths in plain: B3LYP; in bold: M05-2X; in italics: BH&H. The yellow arrow represents the normal vector (τ_C) of the plane defined by N1N3C5 of C, and the orange arrow represents the vector (τ_G) of the plane defined by N1N3C5 of G.

Results and Discussion

Geometries:

Base–base stacking: The fully optimized geometries of the neutral and anionic tetrahydrated dinucleoside phosphates are depicted in Figures 1 and 2, and the corresponding geometric parameters of the base-stacking are listed in Table 1. Taking the dispersion interaction into account, the M05-2X and the BH&H approaches yield very similar stacking parameters for the optimized structures of the complexes. It is interesting to mention that although the B3LYP approach is not able to describe the dispersion interactions between the nucleobases, it predicts hydrogen-bonding parameters quite close to those deduced by the M05-2X functional. On the other hand, the hydrogen-bond lengths resulting from the BH&H method are systematically about 0.1 to 0.2 Å shorter than those from the B3LYP and M05-2X approaches. The following discussion will be based on the M05-2X results, and the BH&H values will be listed in parentheses.

In its neutral form, guanine stacks over cytosine with a base–base angle (θ, see Figure 1 and Table 1) of 10.9° in the dGpdC system (with both M05-2X and BH&H approaches). The base–base distance (the distance between the center of cytosine and the plane of guanine (R)) is 3.36 Å with the M05-2X method, and 3.21 Å with the BH&H method for this complex. In parallel, the base–base angle is 22.5° (22.3°) and the base–base distance is 3.53 Å (3.42 Å) for dCpdG (Figure 2 and Table 1). These base–base distances accord well with those found in DNA and RNA structures (≈3.4 Å[87]). Electron attachment to the dinucleoside phosphates significantly increases the base–base angle to 29.7° (29.6°) for $[dGpdC]^{\bullet-}$ and 25.9° (25.1°) for $[dCpdG]^{\bullet-}$. Meanwhile, an excess electron residing on dGpdC and dCpdG barely influences the base–base distance: R is 3.35 Å (3.16 Å) for the former and 3.48 Å (3.42 Å) for the latter. These variations strongly suggest that electron attachment

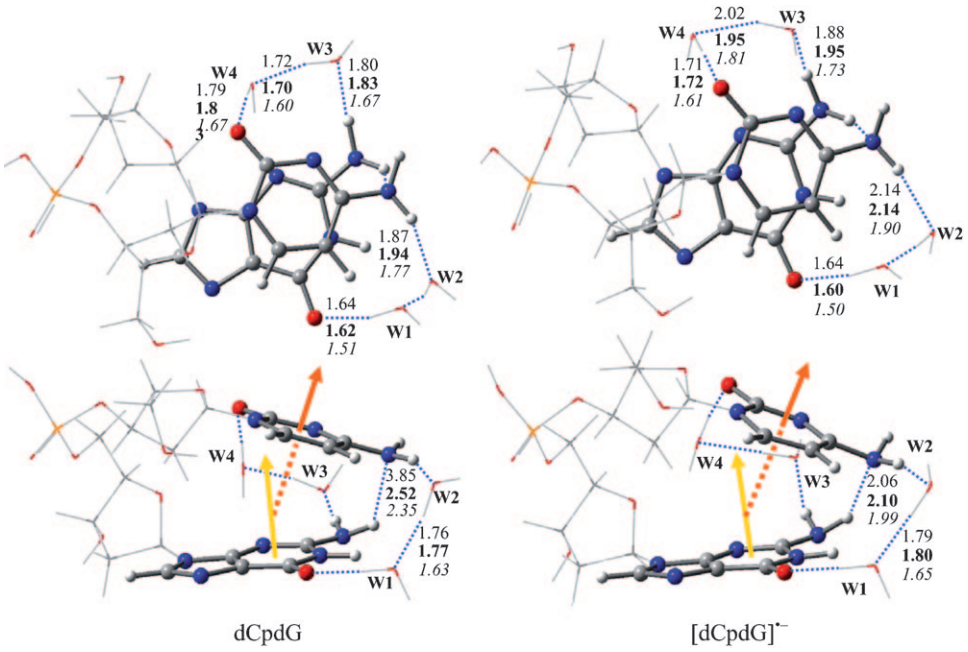

Figure 2. Optimized geometrical structures for the neutral molecules and radical anions of the water microsolvated dCpdG. Bond lengths are in Å. Color representations: orange for P, gray for C, red for O, blue for N, and white for H. The thin lines represent the riboses, the phosphates, and the hydration water molecules. Bond lengths in plain: B3LYP; in bold: M05-2X; in italics: BH&H. The yellow arrow represents the normal vector (τ_C) of the plane defined by N3N1C5 of C, and the orange arrow represents the vector (τ_G) of the plane defined by N3N1C5 of G.

Table 1. Geometric parameters of the stacked bases in the oligomers.

	Functional	dGpdC	[dGpdC]•−	dCpdG	[dCpdG]•−
θ[a]	B3LYP	6.4	43.2	14.6	32.9
	BH&H	10.9	29.6	22.3	25.1
	M05-2X	10.9	29.7	22.5	25.9
R[a]	B3LYP	4.10	3.65	4.24	3.93
	BH&H	3.21	3.16	3.42	3.42
	M05-2X	3.36	3.35	3.53	3.48

[a] θ [°] is the angle between the normal vector (τ_G) of the plane defined by N1N3C5 of G and the vector (τ_C) of the plane defined by N1N3C5 of C in dGpdC and [dGpdC]•−. These two planes are defined by N3N1C5 of G and C in dCpdG and [dCpdG]•−. R [Å] is the distance between the geometric center of N1N3C5 of C (O_C) and the plane of G.

to nucleic acid oligomers might slightly disrupt the π stacking between the nucleobases. However, the electron attachment to dGpdC and dCpdG does reinforce the inter-base proton accepting–donating interactions. The H(N2(C))···O2(G) atomic distance decreases from 2.80 Å (2.70 Å) in dGpdC to 2.13 Å (2.04 Å) for [dGpdC]•−. Similarly, The N4(C))···H(N2(G)) atomic distance of 2.52 Å (2.35 Å) in dGpdC is reduced to 2.10 Å (1.99 Å) in [dCpdG]•−.

Due to their inability to describe the dispersion interactions, conventional density functional methods such as B3LYP are widely thought to be incapable of properly predicting stacking geometric features. However, the stable structures of the stacked bases predicted by the B3LYP approach in the present DFT study suggest that the hydrogen-bonding network, through the microsolvating water molecules linking the neighboring bases, may be an important factor in the stabilization of the stacked bases. Relatively large base–base distances (≈4 Å for the neutral species) are partly due to the slight base-base repulsion by the B3LYP approach. It should be noted that the base–base angle is greatly increased (up to 40°) in the radical anions of dGpdC and dCpdG, as predicted at the B3LYP/DZP++ level of theory. The reduced base–base distance (3.65 Å for dGpdC and 3.93 Å for dCpdG) for these two radical anions should not be interpreted as an increasing of the π stacking between the nucleobases; rather, it is a consequence of the enhancement of the inter-base proton accepting–donating interactions. This is clear from the greatly reduced H(N2(C))···O2(G) atomic distance in [dGpdC]•− (3.90 vs. 1.99 Å) and the significantly shortened N4(C))···H(N2(G)) atomic distance (3.85 vs. 2.06 Å) in [dCpdG]•−.

Hydration pattern: Two water molecules (W1 and W2) form a hydrogen-bonding network bridging N7 and O6 of guanine and H(N4) of cytosine in dGpdC (in which W1 donates protons to N7 and O6 of G, and accepts one proton from W2, and W2 accepts one proton H(N4) from cytosine to form the hydrogen-bonding network). Acting both as proton donor and acceptor, another water dimer (W3 and W4) bonds to H(N2) of guanine and O2 of cytosine through hydrogen bonding. These hydration patterns are essentially unaffected by the electron attachment to the dinucleoside phosphate. However, with the presence of the excess electron on the nucleotide dimer, the proton-accepting ability of the nucleobases increases significantly. At the M05-2X level of theory, the hydrogen-bond lengths of H(W4)···O2(C) and H(W1)···O6(G) reduce from 1.74 and 1.97 Å in dGpdC to 1.57 and 1.87 Å in [dGpdC]•−, respectively. Meanwhile, the electron attachment to the nucleobases decreases their proton donating ability. The hydrogen bonds H(N4(C))···O(W2) of 1.82 Å and H(N2(G))···O(W3) of 1.87 Å in the neutral complex elongate to 2.14 and 2.02 Å, respectively, in the corresponding radical anion.

The hydrogen-bonding network in dCpdG consists of a water dimer (W1 and W2) linking to O6 of G and H(N4) of C, and the other water dimer (W3 and W4) bridging H(N2) of G and O2 of C. Both water dimers act as proton donors

and acceptors here. Similar to dGpdC, electron attachment to dCpdG alters the proton accepting and donating abilities. The enhancement of proton-accepting ability is revealed by the shortened hydrogen bond H(W4)···O2(C) in $[dCpdG]^{\bullet-}$ (the distance is 1.72 Å, whereas it is 1.83 Å in dCpdG). The weakened proton-donating ability of the radical anion of dinucleoside phosphate is signified by the elongated hydrogen bonds H(N2(G))···O(W3) (1.95 Å in $[dCpdG]^{\bullet-}$ vs. 1.83 Å in dCpdG) and H(N4(C))···O(W2) (2.14 Å in $[dCpdG]^{\bullet-}$ vs. 1.94 Å in dCpdG).

It should be noted that the influences of electron attachment to the dinucleoside phosphates on the variations of hydrogen-bond lengths are more pronounced for the cytosine-related hydrogen bonds than for guanine. This difference indicates that cytosine should be the main host of the excess electron in the radical anions of dGpdC and dCpdG.

Electron affinities: The positive electron affinities (Table 2) of the model systems suggest that both dGpdC and dCpdG have strong tendencies to capture excess electrons and to form electronically stable radical anions.

At the B3LYP/DZP++ level of theory, the adiabatic electron affinities of the microsolvated dGpdC and dCpdG are predicted to be 0.66 and 0.90 eV, respectively. The notable AEA difference between 3′-dCMP and 5′-dCMP (0.33 vs. 0.20 eV)[43,45] is enlarged for dCpdG and dGpdC (0.90 vs. 0.66 eV). Compared to the 5′-phosphated nucleotide 5′-dCMP (AEA = 0.20 eV[43]), the presence of the neighboring guanosine and water microsolvation increase the AEA by 0.46 eV in dGpdC. Similarly, this increase is 0.57 eV for dCpdG (0.90 vs. 0.33 eV for 3′-dCMP[45]). It should be noted that only two water molecules are directly attached to each of the base moieties of the oligonucleotide dimers and the cytosine in these systems. In that sense, the latter systems may be viewed as principally dihydrated. Note that the largest AEA increase due to the dihydration of cytosine is 0.50 eV.[69] The influence of the neighboring guanosine is expected to improve the electron-capturing ability of cytosine by about 0.07 eV at most.

Taking the dispersion interaction into account, the M05-2X functional predicts the AEAs of C (−0.11 eV), dGpdC (0.64 eV), and dCpdG (0.90 eV) very close to those yielded by the B3LYP approach. In comparison, the BH&H functional systematically underestimates the electron affinities of these complexes by about 0.3 eV (−0.41 eV for C, 0.32 eV for dGpdC, and 0.62 eV for dCpdG). Three different functionals, with or without considering the dispersion interaction, all yield similar AEA increases from nucleobase (C) to nucleotide dimers (dGpdC and dCpdG): 0.75 eV by M05-2X, 0.73 eV by BH&H, and 0.75 eV by B3LYP for dGpdC; 1.01 eV by M05-2X, 0.92 eV by BH&H, and 0.99 eV by B3LYP for dCpdG. Therefore, the π-stacking interaction between nucleobases G and C seems unlikely to improve the electron-capturing ability of the oligonucleotide dimers. The influence of the neighboring base on the electron-capturing ability of cytosine should be attributed to the intensified proton accepting–donating interaction between the bases, as revealed in the discussion of the geometries above.

The influence of the existence of the neighboring guanosine nucleotide on the electron affinity of cytidine is obviously different. Whereas the guanosine nucleotide on the 5′ position of cytidine (dGpdC) increases the AEA of dC to 0.66 eV, the guanosine nucleotide on the 3′ position of dC (dCpdG) raises the AEA up to 0.90 eV.

To explore the electron-capturing behavior of DNA single strands at the nascent stage of electron attachment, it is important to estimate the VEAs. The near zero VEAs predicted for the microsolvated oligonucleotide dimers (0.25 eV for dGpdC and 0.16 eV for dCpdG by the B3LYP functional, −0.11 eV for dGpdC and −0.17 eV for dCpdG by the M05-2X functional, and −0.26 eV for dGpdC and −0.37 eV for dCpdG by the BH&H functional) in the present investigation indicate that the cytosine- and guanine-rich nucleotide oligomers are reasonable electron captors for low-energy electrons. In comparison, relatively small VEA values have been estimated by the B3LYP approach for 3′,5′-dCDP (0.03 eV), 3′-dCMP (0.15 eV), and 5′-dCMP (−0.11 eV). The

Table 2. Electron affinities of nucleic acid bases, nucleosides, nucleotides, and oligonucleotides [in eV]. The notation C*n*w ($n = 1$ to 5) describes the cytosine anion microsolvated with n water molecules. Results obtained with the B3LYP functional: plain print; M05-2X: **bold**; BH&H: *italics*.

Process	AEA	VEA[a]	VDE[b]
dGpdC→$[dGpdC]^{\bullet-}$	0.66, **0.64**, *0.32*	0.25, **−0.11**, *−0.26*	1.42, **1.50**, *1.20*
dCpdG→$[dCpdG]^{\bullet-}$	0.90, **0.90**, *0.62*	0.16, **−0.17**, *−0.37*	1.64, **1.61**, *1.31*
3′,5′-dGDP→$[3′,5′\text{-dGDP}]^{\bullet-}$	0.24[c]	0.14[c]	0.32[c]
3′,5′-dCDP→$[3′,5′\text{-dCDP}]^{\bullet-}$	0.27[c]	0.03[c]	0.71[c]
3′-dCMP→$[3′\text{-dCMP}]^{\bullet-}$	0.33[d]	0.15[d]	1.28[d]
5′-dCMP→$[5′\text{-dCMP}]^{\bullet-}$	0.20[e]	−0.11[e]	0.85[e]
dG:dC→$dG:dC^{\bullet-}$	0.83[f]	0.16[f]	
G:C→$G:C^{\bullet-}$	0.60[g]	0.03[g]	
dG→$dG^{\bullet-}$	0.01[h]		0.05[h]
dC→$dC^{\bullet-}$	0.21[h]	−0.09[h]	0.72[h]
G→$G^{\bullet-}$	−0.14[i]		
C→$C^{\bullet-}$	−0.09,[i] **−0.11**,[j] *−0.41*[j]		
C1w→$[C1w]^{\bullet-}$	0.16, 0.07–0.18[k]		0.15–0.93[k]
C2w→$[C2w]^{\bullet-}$	0.29, 0.03–0.41[k]		0.22–1.21[k]
C3w→$[C3w]^{\bullet-}$	0.39, 0.08–0.49[k]		0.19–1.54[k]
C4w→$[C4w]^{\bullet-}$	0.41, 0.17–0.50[k]		0.39–1.68[k]
C5w→$[C5w]^{\bullet-}$	0.44, 0.12–0.46[k]		0.41–1.65[k]

[a] $VEA = E_{neutral} - E_{anion}$; the energies are evaluated using the optimized neutral structures. [b] $VDE = E_{neutral} - E_{anion}$; the energies are evaluated using the optimized anion structures. [c] Reference [48]. [d] References [44,45],in which 3′-dCMP was labeled as 3′-dCMPH. [e] Reference [43], in which 5′-dCMP was labeled as 5′-dCMPH. [f] Reference [54]. [g] Reference [52]. [h] Reference [37]. [i] Reference [39]. [j] This research. [k] Reference [69].

notable increase in the VEAs of the microsolvated oligonucleotide dimers suggests that the existence of the neighboring guanosine and water microsolvation improve the effective electron-capturing abilities for cytosine-derived DNA single strands.

The vertical detachment energies (VDE) are the energetic properties most readily observed by the critically important anion photodetachment experiments.[27,34,36] The VDEs of the radical anions of the oligonucleotides dGpdC and dCpdG have been predicted here in order to evaluate their electronic stability. The VDEs are found to be 1.42 eV for $[dGpdC]^{\bullet-}$ and 1.64 eV for $[dCpdG]^{\bullet-}$, significantly larger than those for the corresponding nucleotides (0.85 eV for $[5'\text{-dCMP}]^{\bullet-}$ and 1.28 eV for $[3'\text{-dCMP}]^{\bullet-}$). Because these VDE values are far larger than that of guanosine diphosphate (0.32 eV), the excess electron is expected to be located mainly on the cytosine moiety in $[dGpdC]^{\bullet-}$ and $[dCpdG]^{\bullet-}$. These large VDEs also ensure that reactions with activation barriers lower than 1.4 eV ($\approx$35 kcal mol^{-1}), such as those for O–C σ bonds[43,45] and N-glycosidic bond breakage,[47] are able to occur without electron detachment for the radical anions of the oligonucleotide.

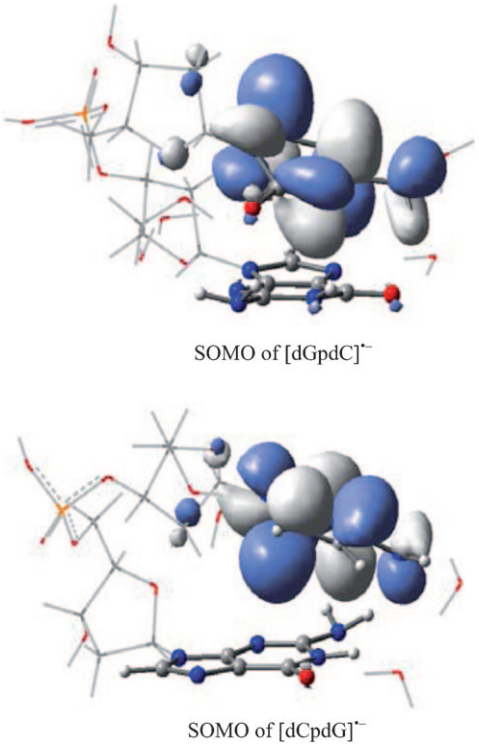

Figure 3. Plots of the singly-occupied molecular orbitals (SOMOs) of the radical anions of dGpdC and dCpdG.

Molecular orbital and charge distribution analysis: Examination of the molecular orbital occupied by each unpaired electron provides a direct electronic-structure-based rationale for the electron-attracting capabilities of the oligonucleotides. Plots of the singly-occupied molecular orbitals (SOMOs) for the radical anions of dGpdC and dCpdG are shown in Figure 3. The most striking feature revealed by the SOMOs of these two dinucleoside phosphate molecules is that the excess electron density resides essentially on the cytosine base moiety.

The location of the negative charge on the constituent parts of the nucleoside pair also provides some insight into the overall electronic effect of the charge. Table 3 summarizes the charge distributions among the bases, ribose, and phosphates for both the neutral and anionic complexes. The analysis of the NPA charge differences between the neutral and anionic oligonucleotides supports the conclusion that the excess electron mainly resides on the cytosine nucleobase moiety in the oligonucleotide radical anions. The NPA charge differences suggest that there is 0.75 to 0.78 a.u. of "negative charge" located on the cytosine, and approximately 0.07 to 0.10 a.u. on the ribose of the cytosine in both dGpdC and dCpdG. It is important to note that about 0.1 a.u. of negative charge is located on the hydration water molecules. The distribution of the "last" electron amongst the constituent parts seems directly correlated with the geometric features discussed above.

Table 3. NPA charge distributions of the neutral molecules and radical anions for the dinucleoside phosphates [in a.u.]. Results obtained here with the B3LYP functional: plain print; M05-2X: **bold**; BH&H: *italics*.

Component	Neutral	Anion	Δ[a]
dCpdG			
G	−0.24, **−0.24**, *−0.25*	−0.27, **−0.26**, *−0.28*	−0.03, **−0.02**, *−0.03*
C	−0.26, **−0.27**, *−0.27*	−1.04, **−1.09**, *−1.07*	−0.78, **−0.82**, *−0.80*
ribose(G)	0.66, **0.68**, *0.68*	0.64, **0.66**, *0.66*	−0.02, **−0.02**, *−0.02*
ribose(C)	0.64, **0.65**, *0.65*	0.57, **0.60**, *0.59*	−0.07, **−0.05**, *−0.06*
phosphate	−0.76, **−0.77**, *−0.77*	−0.79, **−0.80**, *−0.79*	−0.03, **−0.03**, *−0.02*
water	−0.04, **−0.05**, *−0.05*	−0.11, **−0.11**, *−0.12*	−0.07, **−0.06**, *−0.07*
dGpdC			
G	−0.25, **−0.26**, *−0.25*	−0.30, **−0.30**, *−0.31*	−0.05, **−0.04**, *−0.06*
C	−0.28, **−0.28**, *−0.28*	−1.03, **−1.07**, *−1.05*	−0.75, **−0.79**, *−0.77*
ribose(G)	0.64, **0.66**, *0.66*	0.64, **0.66**, *0.64*	0.00, **0.00**, *−0.02*
ribose(C)	0.65, **0.66**, *0.66*	0.55, **0.58**, *0.59*	−0.10, **−0.08**, *−0.07*
phosphate	−0.76, **−0.77**, *−0.76*	−0.77, **−0.78**, *−0.77*	−0.01, **−0.01**, *−0.01*
water	0.00, **0.00**, *−0.01*	−0.09, **−0.09**, *−0.10*	−0.09, **−0.09**, *−0.09*

[a] NPA charge difference between analogous neutral and anionic species.

Effects of solvation: Analogous to the pyrimidine monophosphates and diphosphates, interaction with water greatly improves the electron-capturing abilities of DNA single strands.[17,43,45,46,48] Note that when we speak of the "electron affinity" of a solvated molecule M, the physical situation described is a microsolvated $M(H_2O)_n$ system, in which the water molecules uniformly enclose M, and n becomes arbitrarily large. Meanwhile, there is no proton exchange be-

tween M and the solvent. In this sense, the "AEA" values are 1.49–1.77 eV for dGpdC and 1.86–2.19 eV for dCpdG (with the three functionals used in this investigation) in aqueous solution (see Table 4). Compared to the microsolvated oligonucleotides, the increases of the AEA in aqueous solution amount to about 1.0–1.3 eV for both dGpdC and dCpdG. Another effect of the solvation is the increasing electronic stability of the radical anions. The VDEs of $[dGpdC]^{\bullet-}$ and $[dCpdG]^{\bullet-}$ rise up to 2.5–2.7 eV in the PCM model. These increases clearly demonstrate that microsolvation with water molecular numbers up to four is still not enough to describe the effects of full solvation on the AEA of DNA single strands.

Table 4. "Electron affinities" of nucleotides [in eV] in aqueous solution. Results obtained here with the B3LYP functional: plain print; M05-2X: **bold**; BH&H: *italics*.

Process	AEA [eV]	VDE [eV]
dGpdC→$[dGpdC]^{\bullet-}$	1.65, **1.77**, *1.49*	2.58, **2.74**, *2.50*
dCpdG→$[dCpdG]^{\bullet-}$	1.91, **2.19**, *1.86*	2.74, **2.84**, *2.58*
3′,5′-dCDP→$[3′,5′\text{-dCDP}]^{\bullet-}$	1.99[a]	
5′-dCMP→$[5′\text{-dCMP}]^{\bullet-}$	1.89[b]	
3′-dCMP→$[3′\text{-dCMP}]^{\bullet-}$	2.18[c]	

[a] Reference [48]. [b] Reference [43]. [c] References [44,45].

Conclusions

Dinucleoside phosphate deoxycytidylyl-3′,5′-deoxyguanosine (dCpdG) and deoxyguanylyl-3′,5′-dexoycytidine (dGpdC) systems are among the minimal length DNA single strands that might be considered representative. Exploring electron attachment to these subunits of DNA single strands brings us significantly closer to reliable predictions for the electron affinities of DNA single strands.

DNA single strands have a strong tendency to host low-energy electrons and to form electronically stable radical anions. The VEAs predicted for dGpdC (−0.26 to 0.25 eV) and dCpdG (−0.37 to 0.16 eV) in this investigation indicate that guanine–cytosine mixed DNA single strands have the ability to capture low-energy electrons. A substantial increase in the AEA is predicted as compared to that of the corresponding nucleoside and nucleotide. The adiabatic electron affinities of the oligonucleotides are sequence dependent. Deoxycytidine on the 5′ end, dCpdG, has a larger AEA (0.90 eV) than dC on the 3′ end of the oligomer (dGpdC, 0.66 eV). The effects of the neighboring base and water microsolvation in stabilizing the radical anions of the DNA components are crucial.

The geometric features, molecular orbital analyses, and charge distribution studies for the radical anions of the cytidine-containing oligonucleotides demonstrate that the excess electron in these anionic systems is located on the cytosine nucleobase moiety (around 80%). About 7% of the negative charge is found to be located near the hydration water molecules in these microsolvated systems. The phosphate group for the oligonucleotides seems unlikely to host the excess electron.

Full aqueous solution dramatically increases the electron-capturing ability of the water-microsolvated oligonucleotides, by up to 1 eV, suggesting that microsolvation with water molecular numbers up to four is not enough to describe the effects of full solvation on the AEA of DNA single strands. This research also reveals that the hydrogen-bonding network through the microsolvating water molecules linking to the neighboring bases might be an important factor in the stabilization of the stacked bases.

Forming base-centered radical anions in DNA single strands might represent one of the pathways leading to either N−C glycosidic bond rupture or C−O σ-bond breakage. The present investigation demonstrates that the VDEs of the radical anions of the oligonucleotides dGpdC and dCpdG are significantly larger than those of the corresponding nucleotides. Consequently, reactions with low activation barriers, such as those for O3′−C3′ σ bond,[45] O5′−C5′ σ bond,[43] and N-glycosidic bond breakage,[47] might be expected for the radical anions of the guanosine–cytosine mixed oligonucleotides.

Acknowledgements

This research was supported by the U.S. National Science Foundation, Grant CHE-0749868. J.G. thanks the Chinese Academy of Sciences for continuing supporting.

[1] B. Boudaiffa, P. Cloutier, D. Hunting, M. A. Huels, L. Sanche, *Science* **2000**, *287*, 1658–1659.
[2] L. Sanche, *Eur. Phys. J. D* **2005**, *35*, 367–390, and references therein.
[3] J. Simons, *Acc. Chem. Res.* **2006**, *39*, 772–779, and references therein.
[4] S. G. Ray, S. S. Daube, R. J. Naaman, *Proc. Natl. Acad. Sci. USA* **2005**, *102*, 15–19.
[5] B. Giese, *Acc. Chem. Res.* **2000**, *33*, 631–636.
[6] H. A. Wagenknecht, *Angew. Chem.* **2003**, *115*, 2558–2565; *Angew. Chem. Int. Ed.* **2003**, *42*, 2454–2460.
[7] T. Carell, C. Behrens, J. Gierlich, *Org. Biomol. Chem.* **2003**, *1*, 2221–2228.
[8] D. Porath, G. Cuniberti, R. D. Felice, *Top. Curr. Chem.* **2004**, *237*, 183–227.
[9] "The Chemical Consequences of Radiation Damage to DNA": D. Becker, M. D. Sevilla in *Advances in Radiation Biology, Vol. 17*, Academic Press: New York, **1993**, pp. 121–180.
[10] S. O. Kelley, J. K. Barton, *Science* **1999**, *283*, 375–381.
[11] M. Ratner, *Nature* **1999**, *397*, 480–481.
[12] X. Pan, P. Cloutier, D. Hunting, L. Sanche, *Phys. Rev. Lett.* **2003**, *90*, 208102.
[13] L. G. Caron, L. Sanche, *Phys. Rev. Lett.* **2003**, *91*, 113201.
[14] Y. Zheng, P. Cloutier, D. Hunting, J. R. Wagner, L. Sanche, *J. Am. Chem. Soc.* **2004**, *126*, 1002–1003.
[15] Y. Zheng, P. Cloutier, D. Hunting, J. R. Wagner, L. Sanche, *J. Chem. Phys.* **2006**, *124*, 064710.
[16] Y. Zheng, J. R. Wagner, L. Sanche, *Phys. Rev. Lett.* **2006**, *96*, 208101.
[17] X. Pan, L. Sanche, *Phys. Rev. Lett.* **2005**, *94*, 198104.
[18] D. B. Hall, R. E. Holmlin, J. K. Barton, *Nature* **1996**, *382*, 731–735.
[19] S. Steenken, *Biol. Chem.* **1997**, *378*, 1293–1297.

[20] G. Taubes, *Science* **1997**, *275*, 1420–1421.
[21] Y. A. Berlin, A. L. Burin, M. A. Ratner, *J. Am. Chem. Soc.* **2001**, *123*, 260–268.
[22] D. Beljonne, G. Pourtois, M. A. Ratner, J. L. Bredas, *J. Am. Chem. Soc.* **2003**, *125*, 14510–14517.
[23] M. Ratner, *Nature* **2000**, *404*, 137–138.
[24] M. A. Huels, I. Hahndorf, E. Illenberger, L. Sanche, *J. Chem. Phys.* **1998**, *108*, 1309–1312.
[25] E. C. M. Chen, E. S. D. Chen, W. E. Wentworth, *Biochem. Biophys. Res. Commun.* **1990**, *171*, 97–101.
[26] J. R. Wiley, J. M. Robinson, S. Ehdaie, E. C. M. Chen, E. S. D. Chen, W. E. Wentworth, *Biochem. Biophys. Res. Commun.* **1991**, *180*, 841–845.
[27] J. Schiedt, R. Weinkauf, D. M. Neumark, E. W. Schlag, *Chem. Phys.* **1998**, *239*, 511–524.
[28] B. F. Parsons, S. Sheehan, T. A. Yen, D. M. Neumark, N. Wehres, R. Weinkauf, *Phys. Chem. Chem. Phys.* **2007**, *9*, 3291–3297.
[29] D. Desfrancois, H. Abdoul-Carime, J. P. Schermann, *J. Chem. Phys.* **1996**, *104*, 7792–7794.
[30] V. Periquet, A. Moreau, S. Carles, J. P. Schermann, C. Desfrancois, *J. Electron Spectrosc. Relat. Phenom.* **2000**, *106*, 141–151.
[31] M. Gutowski, I. Dabkowska, J. Rak, S. Xu, J. M. Nilles, D. Radisic, K. H. Bowen, *Eur. Phys. J. D* **2002**, *20*, 431–439.
[32] M. Haranczyk, M. Gutowski, X. Li, K. H. Bowen, *Proc. Natl. Acad. Sci. USA* **2007**, *104*, 4804–4807.
[33] M. Haranczyk, M. Gutowski, X. Li, K. H. Bowen, *J. Phys. Chem. B* **2007**, *111*, 14073–14076.
[34] D. Radisic, K. H. Bowen, I. Dabkowska, P. Storoniak, J. Rak, M. Gutowski, *J. Am. Chem. Soc.* **2005**, *127*, 6443–6450.
[35] N. A. Richardson, S. S. Wesolowski, H. F. Schaefer, *J. Phys. Chem. B* **2003**, *107*, 848–853.
[36] S. T. Stokes, X. Li, A. Grubisic, Y. J. Ko, K. H. Bowen, *J. Chem. Phys.* **2007**, *127*, 084321.
[37] N. A. Richardson, J. Gu, S. Wang, Y. Xie, H. F. Schaefer, *J. Am. Chem. Soc.* **2004**, *126*, 4404–4411.
[38] M. Haranczyk, M. Gutowski, *Angew. Chem.* **2005**, *117*, 6743–6746; *Angew. Chem. Int. Ed.* **2005**, *44*, 6585–6588.
[39] S. S. Wesolowski, M. L. Leininger, P. N. Pentchev, H. F. Schaefer, *J. Am. Chem. Soc.* **2001**, *123*, 4023–4028.
[40] X. Li, M. D. Sevilla, L. Sanche, *J. Am. Chem. Soc.* **2003**, *125*, 8916–8920.
[41] F. Ban, M. J. Lundqvist, R. J. Boyd, L. A. Eriksson, *J. Am. Chem. Soc.* **2002**, *124*, 2753–2761.
[42] J. C. Rienstra-Kiracofe, G. S. Tschumper, H. F. Schaefer, S. Nandi, G. B. Ellison, *Chem. Rev.* **2002**, *102*, 231–282.
[43] X. Bao, J. Wang, J. Gu, J. Leszczynski, *Proc. Natl. Acad. Sci. USA* **2006**, *103*, 5658–5663.
[44] J. Gu, Y. Xie, H. F. Schaefer, *J. Am. Chem. Soc.* **2006**, *128*, 1250–1252.
[45] J. Gu, J. Wang, J. Leszczynski, *J. Am. Chem. Soc.* **2006**, *128*, 9322–9323.
[46] J. Gu, Y. Xie, H. F. Schaefer, *ChemPhysChem* **2006**, *7*, 1885–1887.
[47] J. Gu, Y. Xie, H. F. Schaefer, *J. Am. Chem. Soc.* **2005**, *127*, 1053–1057.
[48] J. Gu, Y. Xie, H. F. Schaefer, *Nucl. Acid Res.* **2007**, *35*, 5165–5172.
[49] X. Li, Z. Cai, M. D. Sevilla, *J. Phys. Chem. B* **2001**, *105*, 10115–10123.
[50] X. Li, Z. Cai, M. D. Sevilla, *J. Phys. Chem. A* **2002**, *106*, 9345–9351.
[51] J. Reynisson, S. Steenken, *Phys. Chem. Chem. Phys.* **2002**, *4*, 5353–5358.
[52] N. A. Richardson, S. S. Wesolowski, H. F. Schaefer, *J. Am. Chem. Soc.* **2002**, *124*, 10163–10170.
[53] J. Gu, Y. Xie, H. F. Schaefer, *J. Phys. Chem. B* **2005**, *109*, 13067–13075.
[54] J. Gu, Y. Xie, H. F. Schaefer, *J. Chem. Phys.* **2007**, *127*, 155107.
[55] J. Gu, Y. Xie, H. F. Schaefer, *J. Phys. Chem. B* **2006**, *110*, 19696–19703.
[56] J. Smets, W. McCarthy, L. Adamowicz, *J. Phys. Chem.* **1996**, *100*, 14655–14660.
[57] J. Smets, D. M. A. Smith, Y. Elkadi, L. Adamowicz, *J. Phys. Chem. A* **1997**, *101*, 9152–9156.
[58] O. Dolgounitcheva, V. G. Zakrzewski, J. V. Ortiz, *J. Phys. Chem. A* **1999**, *103*, 7912–7917.
[59] A. Morgado, K. Pichugin, L. Adamowicz, *Phys. Chem. Chem. Phys.* **2004**, *6*, 2758–2762.
[60] A. Kumar, P. C. Mishra, S. Suhai, *J. Phys. Chem. A* **2005**, *109*, 3971–3979.
[61] X. Bao, H. Sun, N. Wong, J. Gu, *J. Phys. Chem. B* **2006**, *110*, 5868–5874.
[62] X. Bao, G. Liang, N. Wong, J. Gu, *J. Phys. Chem. A* **2007**, *111*, 666–672.
[63] A. O. Colson, B. Besler, M. D. Sevilla, *J. Phys. Chem.* **1993**, *97*, 13852–13859.
[64] M. D. Sevilla, B. Besler, A. O. Colson, *J. Phys. Chem.* **1994**, *98*, 2215.
[65] J. H. Hendricks, S. A. Lyapustina, H. L. de Clercq, K. H. Bowen, *J. Chem. Phys.* **1998**, *108*, 8–11.
[66] M. L. Nugent, L. Adamowicz, *Mol. Phys.* **2005**, *103*, 1467–1472.
[67] S. Kim, H. F. Schaefer, *J. Chem. Phys.* **2006**, *125*, 144305.
[68] S. Kim, S. E. Wheeler, H. F. Schaefer, *J. Chem. Phys.* **2006**, *124*, 204310.
[69] S. Kim, H. F. Schaefer, *J. Chem. Phys.* **2007**, *126*, 064301.
[70] M. Kobylecka, J. Jeszczynski, J. Rak, *J. Am. Chem. Soc.* **2008**, *130*, 15683–15687.
[71] J. Simons, *Acc. Chem. Res.* **2006**, *39*, 772–779, and references therein.
[72] A. D. Becke, *J. Chem. Phys.* **1993**, *98*, 5648–5652.
[73] C. Lee, W. Yang, R. G. Parr, *Phys. Rev. B* **1988**, *37*, 785–789.
[74] A. D. Becke, *J. Chem. Phys.* **1993**, *98*, 1372–1377.
[75] Y. Zhao, D. G. Truhlar, *Acc. Chem. Res.* **2008**, *41*, 157–167.
[76] Y. Zhao, N. E. Schultz, D. G. Truhlar, *J. Chem. Theory Comput.* **2006**, *2*, 364–382.
[77] T. H. Dunning, *J. Chem. Phys.* **1970**, *53*, 2823–2833.
[78] T. J. Lee, H. F. Schaefer, *J. Chem. Phys.* **1985**, *83*, 1784–1794.
[79] M. Cossi, V. Barone, R. Cammi, J. Tomasi, *Chem. Phys. Lett.* **1996**, *255*, 327–335.
[80] A. E. Reed, P. R. Schleyer, *J. Am. Chem. Soc.* **1990**, *112*, 1434–1445.
[81] A. E. Reed, L. A. Curtiss, F. Weinhold, *Chem. Rev.* **1988**, *88*, 899–926.
[82] Gaussian 03 (Revsion E. 01), M. J. Frisch, G. W. Trucks, H. B. Schlegel, G. E. Scuseria, M. A. Robb, J. R. Cheeseman, J. A. Montgomery Jr., T. Vreven, K. N. Kudin, J. C. Burant, J. M. Millam, S. S. Iyengar, J. Tomasi, V. Barone, B. Mennucci, M. Cossi, G. Scalmani, N. Rega, G. A. Petersson, H. Nakatsuji, M. Hada, M. Ehara, K. Toyota, R. Fukuda, J. Hasegawa, M. Ishida, T. Nakajima, Y. Honda, O. Kitao, H. Nakai, M. Klene, X. Li, J. E. Knox, H. P. Hratchian, J. B. Cross, C. Adamo, J. Jaramillo, R. Gomperts, R. E. Stratmann, O. Yazyev, A. J. Austin, R. Cammi, C. Pomelli, J. W. Ochterski, P. Y. Ayala, K. Morokuma, G. A. Voth, P. Salvador, J. J. Dannenberg, V. G. Zakrzewski, S. Dapprich, A. D. Daniels, M. C. Strain, O. Farkas, D. K. Malick, A. D. Rabuck, K. Raghavachari, J. B. Foresman, J. V. Ortiz, Q. Cui, A. G. Baboul, S. Clifford, J. Cioslowski, B. B. Stefanov, G. Liu, A. Liashenko, P. Piskorz, I. Komaromi, R. L. Martin, D. J. Fox, T. Keith, M. A. Al-Laham, C. Y. Peng, A. Nanayakkara, M. Challacombe, P. M. W. Gill, B. Johnson, W. Chen, M. W. Wong, C. Gonzalez, J. A. Pople, Gaussian, Inc., Pittsburgh, PA, **2004**.
[83] M. P. Waller, A. Robertazzi, J. A. Platts, D. E. Hibbs, P. A. Williams, *J. Comput. Chem.* **2006**, *27*, 491–504.
[84] S. D. Wetmore, R. J. Boyd, L. A. Eriksson, *Chem. Phys. Lett.* **2000**, *322*, 129–135.
[85] N. Russo, M. Roscano, A. Grand, *J. Comput. Chem.* **2000**, *21*, 1243–1250.
[86] R. A. Bachorz, W. Klopper, M. Gutowski, *J. Chem. Phys.* **2007**, *126*, 085101.
[87] W. Saenger, *Principles of Nucleic Acid Structure*, Springer, New York, **1983**.

Received: October 28, 2009
Published online: March 26, 2010

